Journal of Alloys and Compounds 509 (2011) 4457–4461

Contents lists available at ScienceDirect

Journal of Alloys and Compounds

journal homepage: www.elsevier.com/locate/jallcom

Variable temperature performance of intermetallic lithium-ion battery anode materials

Andrew N. Jansen, Jessica A. Clevenger, Anna M. Baebler, John T. Vaughey*

Electrochemical Energy Storage Group, Chemical Sciences and Engineering Division, Argonne National Laboratory, Argonne, IL 60439, United States

ARTICLE INFO

Article history:
Received 9 November 2010
Received in revised form 7 January 2011
Accepted 16 January 2011
Available online 22 January 2011

Keywords:
Lithium ion battery
Anode
Low temperature
Intermetallic

ABSTRACT

Although a variety of cathode and electrolyte materials have been studied and commercialized over the past two decades, nearly all commercial cells have used a graphitic carbon anode. Several reasons exist for this choice—including cost, low insertion voltage, and ease of use in the cell manufacturing process. However as uses for lithium-ion batteries expand, alternative anodes that may offer better energy and power capability are being explored. For transportation-oriented purposes, anodes based on simple lithiated Zintl compounds, e.g. $Li_{17}Sn_4$, or intermetallic insertion anodes offer significant advantages in capacity (volumetric and gravimetric) and stability in the cell environment that make them attractive candidates for future cell chemistries. Within this context, little however is known about how these alternative anode materials perform as a function of temperature, which is important for applications where operation at temperatures as low as −30 °C can be expected. In this study we evaluated a series of intermetallic insertion anodes that operate by a simple metal displacement mechanism. We have found that for Cu_6Sn_5, Ag/Cu_6Sn_5, and Cu_2Sb, the drop-off in performance with temperature is in line with that observed for a commercial graphite-based anode and indicates that additional variables such as cation diffusion through the electrode passivation film or the electrochemical double layer may be playing an important role that is independent of the underlying anode material. We additionally characterized the NiAs-type mineral Sorosite ($CuSn_{0.9}Sb_{0.1}$), as various literature reports had indicated that substitution of antimony for tin eliminated the need for interstitial copper, however powder X-ray diffraction studies of samples made by annealing or high energy ball milling indicated mixed phase samples.

1. Introduction

As lithium-ion batteries expand into more markets, requirements for the battery and the environment they operate in will change to meet the new demands. Among the most discussed new markets for Li-ion batteries are electric vehicles (EVs), hybrid electric vehicles (HEVs) and plug-in hybrid electric vehicles (PHEVs). Besides requirements for power and energy, the ability for the battery to work over a wide temperature range has been identified as an important variable requiring optimization [1]. For automobiles, manufacturers have proposed that the battery used be required to operate over the temperature range from −30 °C to 52 °C. Either temperature extreme has unique problems associated with it that can lead to shortened lifetimes or battery failure. For state of the art systems based on a graphitic carbon anode, higher cycling temperatures produces problems that lead to poor cycling performance including destabilization of the surface electrolyte interphase (SEI) layer, electrolyte salt breakdown, changes in lithium transport kinetics, and increased surface reactivity [2–6]. To combat these problems electrode coatings deposited before lamination and electrolyte additives that polymerize to a protective film at a specific voltage have been used to stabilize and control the interface between the electrolyte and active electrode to enable the use of graphitic carbons [2]. However at low temperatures, electrolyte constituent stability issues have not been implicated as the cause of the cycling problems, instead aspects of the lithium cation diffusivity and stability of the electrode/electrolyte interface have been postulated as sources of cell failure [5–12]. Whereas electrolyte formulations that work well at low temperatures have been reported, notably by the aerospace industry, most have been optimized for slow discharge applications which may not be transferable to the transportation sector where power requirements are higher [7–9,11].

Most variable temperature electrode studies in the literature have focused on commercialized intercalation anodes, such as graphite or the spinel $Li_4Ti_5O_{12}$ [13]. However several alternative anode systems, including ones based on alkali metal Zintl

* Corresponding author. Tel.: +1 630 252 8885.
E-mail address: vaughey@anl.gov (J.T. Vaughey).

0925-8388/$ – see front matter © 2011 Published by Elsevier B.V.
doi:10.1016/j.jallcom.2011.01.111

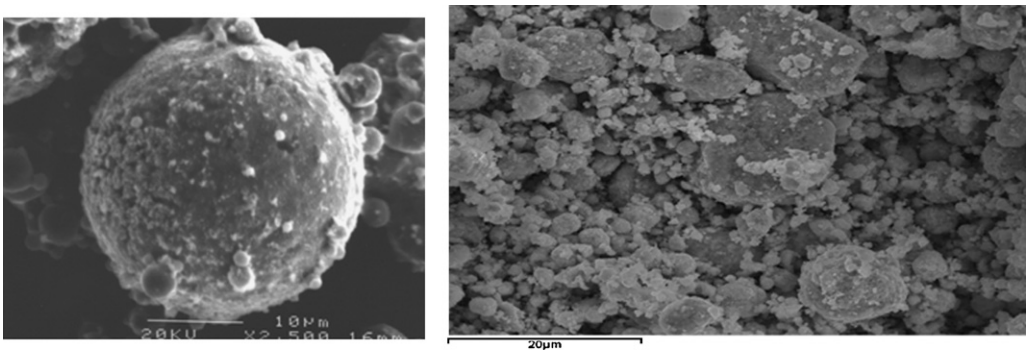

Fig. 1. SEM images of the (a) Ag-coated Cu_6Sn_5 sample, and (b) high energy ball milled Cu_2Sb.

compounds, metal oxide displacement, and intermetallic insertion reactions, are under investigation for the next generation of lithium-ion batteries. Of these alternatives, intermetallic insertion anodes, systems that reversibly store lithium in the form of ternary lithium intermetallic compounds, have been shown to have capacities up to twice that of graphitic carbon in approximately one half the volume while maintaining a low insertion voltage. This high volumetric capacity is useful for devices where space is at a premium. A representative example of this class of materials is the intermetallic compound Cu_6Sn_5, a superstructure type in the NiAs–Ni_2In family of compounds [14,15]. Experimental and theoretical studies show that on initial charge (lithiation down to 0.5 V) the compound inserts approximately 3 lithium cations topotactically to form $Li_3[Cu_6Sn_5]$, also on the NiAs–Ni_2In line. Further lithiation (down to 0.3 V) results in a two-phase plateau with formation of Li_2CuSn (Cu_2MnAl-type) with displacement of 16% of the copper to the grain boundaries. Further lithiation results in copper displacement and isolation of Li_xSn Zintl phases [16]. Charging the samples (removing lithium) results in re-formation of the Li_2CuSn intermediate initially and eventually Cu_6Sn_5, although a point in the solid solution, e.g. $(Cu_{6-x}Li_x)Sn_5$, cannot been eliminated as a possibility [17]. The copper needed for Cu_6Sn_5 re-formation at top of charge is thought to come from a combination of the copper displaced to the grain boundaries and the copper current collector (corrosion), as well as formation of a defect structure that may still contain residual lithium [17–19]. For intermetallic insertion anode materials, high reversible capacities have been observed at room temperature, however there are no reports on the effects of temperature on cycling. In this study we have assessed the variable temperature performance of several intermetallic insertion anode materials where lithium storage mechanism is based on reversible metal displacement. In this way we hope to get a better understanding of how the reverse reaction, re-incorporation of the displaced metal into the structure, is affected by the changes that occur in the electrochemical cell as the temperature is lowered. A key factor, when comparing to graphite anodes, is the ability of the lithium to be transported across the SEI layer and into the negative electrode. The solid-electrolyte-interphase (SEI) layer is a type of passivation layer formed on the surface of the electrode at low voltages by the reaction of the negative electrode and the electrolyte components. In general the SEI layer on intermetallic anodes is richer in inorganic salts and contains less organic salts and electrolyte-derived oligomers than those found on graphite [20–22]. It has been speculated that these organic oligomers are better at conducting lithium than the inorganic salts as the temperature is lowered and thus poorer electrode performance should be expected [20]. In this study, the variable temperature rate capability of Cu_6Sn_5, Cu_2Sb, and Ag-coated Cu_6Sn_5 electrodes was evaluated and compared to a commercial graphitic carbon.

2. Experimental details

2.1. Materials synthesis

The intermetallic compound Cu_6Sn_5 was obtained from Polystor Corp., and was used as received. Silver coated Cu_6Sn_5 was made by a variation of the analytical Tollen's test used to detect aldehydes. A sample of Cu_6Sn_5 was suspended in an aqueous solution of $AgNO_3$ (5 wt% relative to alloy). While being stirred vigorously, a stoichiometric excess of formaldehyde was added to the solution resulting in the instantaneous reduction of the silver ions to metallic silver which adheres primarily to the surface of the suspended alloy particles. Cu_2Sb was prepared by the reaction of a stoichiometric mixture of the elements using a high energy ball mill (HEBM) as previously reported [23]. Each of the alloys was characterized by SEM, powder XRD, and electrochemical methods prior to use. Fig. 1 shows the scanning electron micrographs (SEM) of the alloys. Fig. 2 shows the powder X-ray diffraction patterns of Cu_6Sn_5 and Ag-coated Cu_6Sn_5. A series of materials based on the reported Sorosite formulation $CuSn_{1-x}Sb_x$ ($0 < x < 0.12$) were synthesized by either direct reaction of the elements at high temperature (800 °C) under an inert atmosphere followed by mechanical grinding or by high energy ball milling (HEBM) of the elements [24,25]. The synthetic graphite powder MAG10 (Hitachi Powdered Metals Co. Ltd.) was used as received in this study as our graphite anode for comparison [12].

2.2. Electrochemical testing

Variable temperature rate evaluations were performed using 2032-type cell hardware (Hohsen) and a lithium metal anode (FMC lithium). The electrolyte was 1.2 M $LiPF_6$ in EC/EMC (3:7). The battery-grade electrolyte was purchased from Tomiyama Pure Chemical Industries (Tokyo, Japan) and analyzed by Karl Fischer titration to contain less than 20 ppm moisture. All cell preparations were handled in an argon-atmosphere glovebox maintained at <1 ppm water and <5 ppm oxygen. Active material laminates were made using 80 wt% active materials, 10 wt% polyvinyl difluoride (PvDF) binder, and 10 wt% acetylene black [23]. Before use laminates were dried at 65 °C in a vacuum drying oven to ensure no moisture was trapped in the pores of the electrode. Capacity and power capability were determined at 30 °C, 0 °C, and −30 °C.

3. Results and discussion

3.1. Insertion mechanism

As commercial markets for lithium-ion batteries increase, the conditions the cells operate under will vary significantly depend-

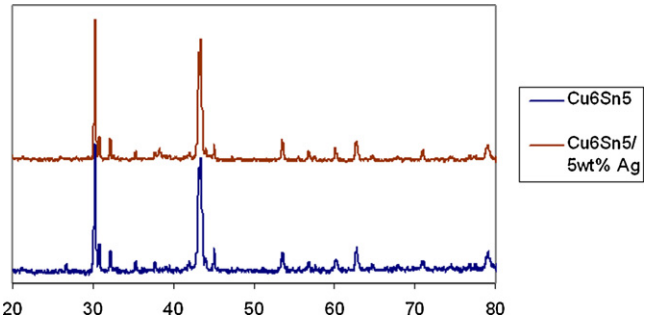

Fig. 2. XRD patterns of the Ag-coated and uncoated Cu_6Sn_5 alloy samples.

ing on the end-users requirements. For automotive applications, requirements include that the battery be capable of operating over a wide temperature range. However when evaluating the power capability, the speed at which lithium can be cycled in and out of the electrode, of common lithium-ion cell chemistries, a dramatic rise in impedance has been observed as the temperature is lowered [7–9]. Whereas numerous studies have sought to improve the variable temperature power performance of graphitic anodes by assessing the effect of particle size reduction, electrolyte additives, or amorphous carbon coatings, equivalent studies on alternative anode materials are hampered by the lack of data on baseline systems needed for comparison [2–9,13]. In this study we evaluated the variable temperature rate capability of a series of intermetallic insertion anode materials that work by a metal displacement storage mechanism. Specifically, we examined a commercial graphite (10 μm), Cu_6Sn_5 (10–20 μm), Ag-coated Cu_6Sn_5 (10–20 μm), and Cu_2Sb (10–30 μm) all with approximately the same particle size [23,26–29]. The electrochemical window used for the electrode materials was limited to the voltage cutoffs where an insertion-displacement reaction occurs and formation of a ternary compound has been reported [16,23,26]. The cell reactions are shown below, reactions (1) and (2).

$$Cu_6Sn_5 + 10Li \Leftrightarrow 5Li_2CuSn + Cu \quad (1)$$

$$5Li_2CuSn + 11.25Li \Leftrightarrow 5Li_{4.25}Sn + 5Cu$$

$$Cu_2Sb + 2Li \Leftrightarrow Li_2CuSb + Cu \quad (2)$$

$$Li_2CuSb + xLi \Leftrightarrow Li_{2+x}Cu_{1-x}Sb + xCu (x \leq 1)$$

Although going to complete lithiation of the intermetallic insertion electrode materials (and complete displacement of the transition metal) has been shown to increase the capacity significantly, it also results in shorter cell life and this part of the cycling profile was not considered in this study [15–17,23]. For the two types of intermetallics considered, the amount of copper displaced is dramatically different and, even though the reactions are reversible, re-establishment of equilibrium at top of charge should be effected by the current utilized. The Ag-coated Cu_6Sn_5 material should operate by the same mechanism as Cu_6Sn_5 and was evaluated to determine if the surface silver increased electrode lithium-ion conductivity, via formation of the heavily lithiated phase $Li_{15}Ag_4$ on discharge, at the particle level [30]. Graphite inserts 0.16 lithium cations per carbon atom and operates purely as an insertion material.

3.2. Materials characterization

As part of this study we sought to investigate a synthetic version of the NiAs-type mineral sorosite, $CuSn_{0.9}Sb_{0.1}$ [24,25]. In theory it should operate in a manner similar to reaction (1) but with no need to extrude interstitial copper at the intermediate discharge step with formation hypothetically of "$Li_2CuSn_{0.9}Sb_{0.1}$". The various reported compositions indicated that substitution of approximately 10% of the Sn with Sb would yield a single phase NiAs-type material with no interstitial copper. However various synthetic attempts around the reported Cu:Sn:Sb ratios yielded only mixed phase materials as determined by powder X-ray diffraction methods containing various amounts of Cu_6Sn_5, Sn, and SnSb, in agreement with the ternary phase diagram. Using a simple NiAs-type lattice as a model and the Sn as an internal standard, we fit the dominant peaks in the powder data XRD pattern to determine the change in lattice constants and unit cell volume as a function of Sb content. The data, shown in Fig. 3, indicates 4–5 at% Sb solubility in the NiAs-type structure, in good agreement with the reported

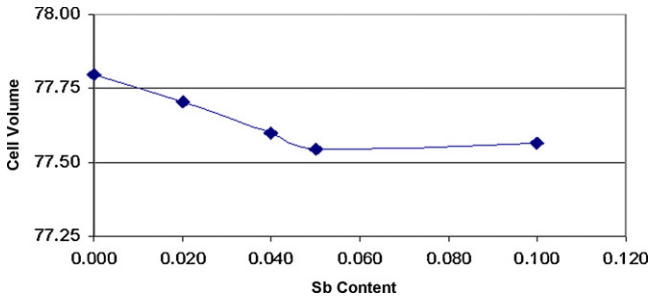

Fig. 3. Plot of NiAs component unit cell volume versus antimony content for the series $Cu(Sn_{1-x}Sb_x)$.

ternary phase diagram showing 3 at% solubility of Sb in Cu_6Sn_5 [31]. Because the loss of interstitial copper by antimony substitution could not be confirmed, the materials were not evaluated electrochemically.

XRD analysis of the commercial Cu_6Sn_5 samples indicated the sample had ~10% extra Sn in the material, which carried over to the Ag-coated sample. This composition has been reported to have slightly better electrochemical performance than single phase Cu_6Sn_5, possibly resulting from the extra Sn either acting to keep the displaced Cu close to the active particle or inhibiting the reaction of the displaced copper with the electrolyte [32]. The coating process did not produce any extra crystalline phases as determined by XRD. SEM/EDX analysis of the coated samples showed a uniform distribution of silver in the sample. The Cu_2Sb was single phase to XRD.

3.3. Electrochemical characterization

For the graphitic carbon (MAG10) samples, the capacity and rate capability as a function of temperature is shown in Fig. 4. At 30 °C, slow discharge (C/5) of the material gave the expected 350 mAh/g (formation of LiC_6) which decreased to 290 mAh/g at C-rate. C-rate is defined as the current necessary to charge the cell in 1 h; a C/2 rate would be a 2 h charging rate. At 0 °C, approximately 67% of the 30 °C capacity was lost, even at the slowest rate, and nearly all of the capacity was lost as the charging time was accelerated. At −30 °C, the electrode had little or no capacity at the rates used. The drop-off in capacity as a function of temperature and rate is in good agreement with previously reported results [7,33].

In Fig. 5, the data was collected for Cu_6Sn_5 and Ag-coated Cu_6Sn_5 electrodes tested in the voltage window (1.2–0.2 V) that limits lithiation approximately to the formation of Li_2CuSn. The materials show the expected capacities (~225 mAh/g; ~1.7 Li/"$Cu_{1.2}Sn$") at 30 °C with little dependence on rate (C/8 to C-rate). The lowest rate 0 °C tests for both show an approximately 33% loss in capacity, while the −30 °C test shows > 90% capacity loss even at the lowest currents used. The Ag-coated sample showed slightly higher elec-

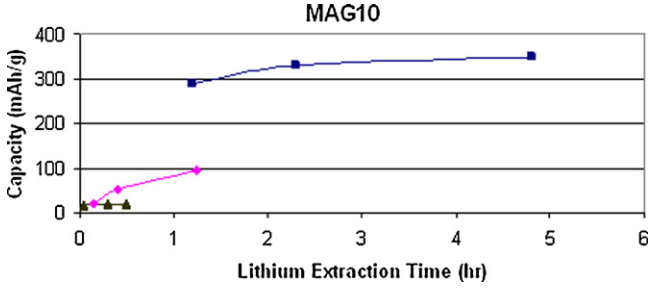

Fig. 4. Variable temperature rate study of MAG-10 graphite. The square data points represent data collected at 30 °C, the diamonds represent data collected at 0 °C, the triangles represent data collected at −30 °C.

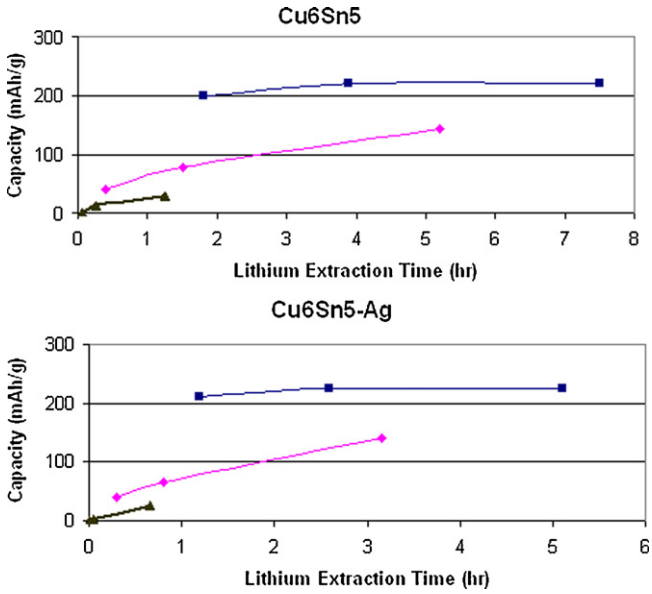

Fig. 5. Variable temperature rate study of Cu_6Sn_5 and Ag-coated Cu_6Sn_5 graphite. The square data points represent data collected at 30 °C, the diamonds represent data collected at 0 °C, the triangles represent data collected at −30 °C.

trode utilization at 30 °C and 0 °C, possibly due to the formation of $Li_{15}Ag_4$ on the surface resulting in an increase in the lithium-ion conductivity of the intermetallic anodes (Cu_6Sn_5) SEI layer. Similar strategies, incorporation of lithium-ion conducting Zintl phases into an SEI layer, have been reported to increase the Li-ion conductivity at lithium metal surfaces [34].

For the Cu_2Sb samples, rate capability as a function of temperature is shown in Fig. 6. At 30 °C, a 30% drop-off in capacity is observed as a function of rate (C/6 to C rate). This may be related to the relatively large amount of copper that must be shuttled into and out of the electrode as the cell is charged and discharged. When compared to the Cu_6Sn_5-based systems, the charge and discharge reactions for Cu_2Sb involve cycling 50% of the available copper in the electrode, versus only 16% for Cu_6Sn_5. As rate is increased, the Cu_2Sb electrode may not be able to reach equilibrium. At 0 °C, approximately 67% of the 30 °C capacity is lost, even at the slowest rate, and nearly all of the capacity is lost as current is increased. At −30 °C, the electrode has little or no capacity.

Numerous studies in the literature have investigated the causes of low temperature power fade in lithium-ion cells that use graphitic anodes. Variables including salt molarity, electrolyte viscosity, electrode binder, conductive additives, and solvent have all been investigated with no definitive identification of the source of the fade [7,9,12]. Reasons cited for the fade with respect to the graphitic carbon anode include poor lithium diffusion within the graphitic layers and decreasing charge transfer characteristics of the surface films [5,11]. In this report we show that there appears to be a universal collapse in power capability as cell temperature is lowered irrespective of lithium storage mechanism. Specifically, the poor low temperature performance of lithium-ion cells cannot be attributed to processes related to the anode material utilized or completely to the electrode/SEI interface, as the SEI layer on intermetallic anodes is significantly enriched in salt decomposition products when compared to graphitic systems [9,10]. Further work studying lithium-based electrolytes as a function of temperature, including de-solvation kinetics, may shed light on this phenomenon and help explain the observed power loss at low temperatures.

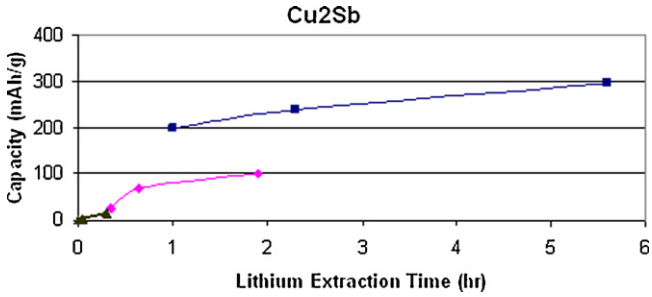

Fig. 6. Variable temperature rate study of Cu_2Sb. The square data points represent data collected at 30 °C, the diamonds represent data collected at 0 °C, the triangles represent data collected at −30 °C.

4. Conclusions

The variable temperature power capability of a variety of lithium-ion battery anodes has been evaluated. At room temperature, all of the anodes performed as expected, however, as the temperature was lowered the energy and power capability of the various types of anodes evaluated, including a synthetic graphite, declined significantly. However since the drop-off in performance is in line with that observed for a commercial graphite-based anode additional variables, including cation diffusion through the SEI layer or the surface double layer, may be playing an important role that is independent of the underlying anode material.

Acknowledgements

J.A.C. and A.M.B. would like to acknowledge the support received while at Argonne National Laboratory as participants in the Science Undergraduate Research Internship (SULI) program administered by the Office of Science: Office of Workforce Development for Teachers and Scientists, U.S. Department of Energy. Support from the Office of Vehicle Technologies (Batteries for Advanced Transportation Technologies Program) of the U.S. Department of Energy under Contract No. DE-AC02-06CH11357 is gratefully acknowledged.

References

[1] V. Srinivasan, AIP Conference Proceedings, vol. 1044, 2008, p. 283.
[2] S. Ota, Y. Sakata, A. Inoue, S. Yamaguchi, J. Electrochem. Soc. 151 (2004) A1659.
[3] A.M. Anderson, K. Edstrom, N. Rao, A. Wendsjo, J. Power Sources 81 (1999) 286.
[4] K. Araki, N. Sato, J. Power Sources 124 (2003) 124.
[5] C.K. Huang, J.S. Sakamoto, J. Wolfenstine, S. Surampudi, J. Electrochem. Soc. 147 (2000) 2893.
[6] T. Abe, H. Fukuda, Y. Iriyama, Z. Ogumi, J. Electrochem. Soc. 151 (2004) A1120.
[7] A.N. Jansen, D.W. Dees, D. Abraham, K. Amine, G.L. Henriksen, J. Power Sources 174 (2007) 373.
[8] D. Abraham, M.M. Furczon, S.H. Kang, D.W. Dees, A.N. Jansen, J. Power Sources 180 (2008) 612.
[9] D. Abraham, J.R. Heaton, S.H. Kang, D.W. Dees, A.N. Jansen, J. Electrochem. Soc. 155 (2008) A41.
[10] K. Xu, Chem. Rev. 104 (2004) 4303.
[11] M.C. Smart, B.V. Ratnakumar, S. Surampudi, J. Electrochem. Soc. 146 (1999) 486.
[12] X.F. Xiang, C.H. Chen, J. Zhang, K. Amine, J. Power Sources 195 (2010) 604.
[13] J.L. Allen, T.R. Jow, J. Wolfenstine, J. Power Sources 159 (2006) 1340.
[14] L. Fransson, E. Nordström, K. Edström, L. Häggström, J.T. Vaughey, M.M. Thackeray, J. Electrochem. Soc. 149 (2002) A736.
[15] J.T. Vaughey, C.S. Johnson, A.J. Kropf, R. Benedek, M. Thackeray, H. Tostmann, T. Sarakonsri, S. Hackney, L. Fransson, K. Edström, J.O. Thomas, J. Power Sources 97–98 (2001) 194.
[16] W. Choi, J.Y. Lee, H.S. Lim, Electrochem. Commun. 6 (2004) 816.
[17] S. Sharma, L. Fransson, E. Sjostedt, L. Nordstrom, B. Johansson, K. Edstrom, J. Electrochem. Soc. 150 (2003) A330.
[18] T. Sarakonsri, T. Apirattanawan, S. Tungprasurt, T. Tunkasiri, J. Mater. Sci. 41 (2006) 4754.
[19] J.J. Zhang, P. He, Y.Y. Xia, J. Electroanal. Chem. 624 (2008) 161.
[20] H.J. Santner, K.C. Moeller, W. Kohs, C. Veit, E. Lanzer, A. Trifonova, M.R. Wagner, P. Raimann, C. Korepp, J.O. Besenhard, in: I.V. Barsukov, C.S. Johnson, J.E. Doninger, V.Z. Barsukov (Eds.), Mathematics, Physics and Chemistry, 2006, 229, 171.

[21] H. Bryngelsson, M. Stjerndahl, T. Gustafsson, K. Edström, J. Power Sources 174 (2007) 970.
[22] M. Stjerndahl, H. Bryngelsson, T. Gustafsson, J.T. Vaughey, M.M. Thackeray, K. Edström, Electrochim. Acta 52 (2007) 4947.
[23] L.F. Fransson, J.T. Vaughey, R. Benedek, K. Edstrom, J.O. Thomas, M.M. Thackeray, Electrochem. Commum. 3 (2001) 317.
[24] A.Y. Barkov, K.V.O. Laajoki, S.S. Gornostayev, Y.A. Pakhomovskii, Y.P. Men'shikov, Am. Mineral. 83 (1998) 901.
[25] S. Lidin, S.Y. Piao, Z. Anorg, Alleg. Chem. 635 (2009) 611.
[26] J.T. Vaughey, J. Owejan, M.M. Thackeray, Electrochem. Solid State Lett. 10 (2007) A220.
[27] I. Kim, J.T. Vaughey, O. Auciello, J. Electrochem. Soc. 155 (2008) A448.
[28] J. Wolfenstine, S. Campos, D. Foster, J. Read, W.K. Behl, J. Power Sources 109 (2002) 230.
[29] H. Bryngelsson, J. Eskhult, L. Nyholm, K. Edstrom, Electrochim. Acta 53 (2008) 7226.
[30] J.T. Vaughey, L. Fransson, H.A. Swinger, K. Edstrom, M.M. Thackeray, J. Power Sources 119 (2003) 64.
[31] J.V. Harding, W.T. Walpole, J. Inst. Met. 75 (1948) 115.
[32] L. Trahey, J.T. Vaughey, H. Kung, M.M. Thackeray, J. Electrochem. Soc. 156 (2009) A385.
[33] Y. Ein-Eli, S.R. Thomas, R. Chadha, T.J. Blakely, V.R. Koch, J. Electrochem. Soc. 144 (1997) 823.
[34] M. Maxfield, T.R. Jow, S. Gould, M.G. Sewchok, L.W. Shacklette, J. Electrochem. Soc. 135 (1988) 299.